JOURNAL PUNJAB ACADEMY OF SCIENCES (Peer Reviewed Open Access Journal)
JPAS, 21: 47-57 (January-December, 2021)
Available online at www.jpas.in
ISSN 2229-7014 (P)

AMORPHOUS SOLIDS IN WATER AND ICE: A REVIEW

Navjot Kaur[1] and Amita[2]
[1]Department of Chemistry, RCCV Girls College, Ghaziabad. UP, India
[2]Department of Chemistry, Baring Union Christian College, Batala, Punjab, India
[1]E-mail:navjotwadhawan@gmail.com
[2]E-mail:dramitabucc@gmail.com

ABSTRACT

Amorphous forms are non-crystalline materials which possess no long-range order. Amorphous solid water is most abundant form of solid water in the universe. Its saturation vapor pressure and thermodynamic properties, however, are still a topic of research by the scholars. We have investigated the saturation vapor pressure over vapor-deposited amorphous ice at temperatures between 133 and 147 K using a novel experimental method (1). The new method determines the absolute vapor pressures and the sublimation rates by measuring the mass growth rates of ice-covered nanoparticles under supersaturated water vapor conditions. It is observed that the vapor pressure of amorphous solid water is up to a factor of 3 higher than that predicted by current parameterizations, which are based in part on calorimetric measurements. The calorimetric measurements can be reconciled with data by acknowledging the formation of nano-crystalline ice as an intermediate ice phase during the crystallization of amorphous ice. The proposed value for the enthalpy of crystallization of amorphous solid water of $\Delta H = 2312 \pm 227$ J/mol, which is about 1000 J/mol higher than the current consensus. The results shine a new light on the abundance of water ice clouds on Mars and mesospheric clouds on Earth and alter our understanding of ice formation in the stratosphere.

Keywords: Amorphous solids, crystalline,Amorphous ice.

INTRODUCTION

Amorphous solid water (ASW) is the most abundant form of solid water in astrophysical environment. It is believed to be a major component of interstellar clouds, comets, and solar-system bodies (2-5). Due to its porosity and capability of adsorbing gases, ASW is discussed to participate as a medium in many chemical reactions in outer space that could play a key role in the earliest stages of planet building (4). However, its true degree of porosity remains unclear due to the lack of unambiguous observational data and a variety of contributing processes during its formation and re-accretion in outer space. ASW was first produced in the laboratory in 1935 by Burton and Oliver through water vapor deposition on a cold copper substrate (6, 7). The so-formed ASW can serve as a model system to better understand part of the contributing processes. Since then, ASW has been intensively studied (8 – 21). The morphologies and physical properties of ASW fabricated in the laboratory can vary with vapor flux and directionality, substrate temperature, and water partial pressure (16, 22-24). The effect of irradiation on the structure of amorphous ice, and in particular on the dangling OH groups, has been studied

using UV (25), IR (18, 26), and heavy ion bombardment (27 – 29). Formation of high-density ASW has been reported to occur at very low deposition temperatures (<30 K). (30-32) When the deposition temperature is increased from 77 to 200 K, the deposited ice phase changes from porous ASW (p-ASW) (2) to collapsed ASW (c-ASW) and eventually to crystalline ice. We note that all of these phases exhibit a low density of around 0.94 g·cm–3 (33-34). The heating process of p-ASW, initially formed at 77 K or below, is accompanied by a pore collapse, hence transforming from p-ASW to c-ASW at temperatures above 120 K (12,22,35,36).

ASW is known to be structurally similar to low-density amorphous ice (LDA) and hyper-quenched glassy water (HGW). All three types of solid water have a first diffraction peak at 1.7 Å–1 in neutron scattering (37) and present a glass transition at around 136 K (38). However, it is not yet fully understood how the p-ASW builds up during vapor deposition nor how the long-range molecular structure changes during the pore collapse.

X-ray diffraction (XRD) and neutron scattering techniques are powerful and non-destructive methods to study molecular-level structures of different materials. They have been previously applied to obtain the structure factors and the pair distribution functions (PDFs) of low- and high-density amorphous ices (LDA and HDA) (38-41).

As ASW is of high astrophysical relevance, most studies investigate the vibrational states via Fourier transform infrared spectroscopy (FTIR), while X-ray and neutron scattering studies are, so far, limited (12,31,35,37). Taking advantage of the high flux of the high-energy X-rays at beamline 6 ID-D of the Advance Photon Source (APS), we were able to perform in situ X-ray measurements on p-ASW during vapor deposition.

The current work presents a combined study of in situ XRD and FTIR on ASW, investigating its formation and the pore collapse during heating. Oxygen–oxygen PDFs of ASW were determined , as a function of temperature , up to 23 Å. The PDFs were then compared with other amorphous ice forms to investigate potential similarities in the long-range ordering. The OH-stretch vibration mode from the FTIR spectrum was recorded as a function of deposition time and temperature, allowing us to follow the changes in the vibrational spectrum

RESULTS AND DISCUSSION

Amorphous solid, any non-crystalline solid in which the atoms and molecules are not organized in a definite lattice pattern. Such solids include glass, plastic, and gel. Solids and liquids are both forms of condensed matter; both are composed of atoms in close proximity to each other. But their properties are, of course, enormously different. While a solid material has both a well-defined volume and a well-defined shape, a liquid has a well-defined volume but a shape that depends on the shape of the container. Stated differently, a solid exhibits resistance to shear stress while a liquid does not. Externally applied forces can twist or bend or distort a solid's shape, but (provided the forces have not exceeded the solid's elastic limit) it "springs back" to its original shape when the forces are removed. A liquid flow under the action of an external force; it does not hold its shape. These macroscopic characteristics constitute the essential distinctions: a liquid flow, lacks a definite shape (though its volume is definite), and cannot withstand a shear stress; a solid does not flow, has a definite shape, and exhibits elastic stiffness against shear stress. On an atomic level, these macroscopic distinctions arise from a basic difference in the nature of the atomic motion. Figure 1 contains schematic representations of atomic movements in a liquid and a solid. Atoms in a solid are not mobile. Each atom stays close to one point in space, although the atom is not stationary but instead oscillates rapidly about this fixed point (the higher the temperature, the faster it oscillates). The fixed point can be viewed as a time-averaged center of gravity of the rapidly jiggling atom.

The spatial arrangement of these fixed points constitutes the solid's durable atomic-scale structure. In contrast, a liquid possesses no enduring arrangement of atoms. Atoms in a liquid are mobile and continually wander throughout the material.

Amorphous Ice: Amorphous ice is an amorphous solid form of water. Common ice is a crystalline material wherein the molecules are regularly arranged in a hexagonal lattice, whereas amorphous ice has a lack of long-range order in its molecular arrangement. Amorphous ice is produced either by rapid cooling of liquid water or by compressing ordinary ice at low temperatures. Although almost all water ice on Earth is the familiar crystalline ice Ih , amorphous ice dominates in the depths of interstellar medium, making this likely the most common structure for H2O in the universe at large. Just as there are many different crystalline forms of ice (currently more than seventeen are known), there are also different forms of amorphous ice, distinguished principally by their densities.

Distinction between crystalline and amorphous solids: There are two main classes of solids: crystalline and amorphous. What distinguishes them from one another is the nature of their atomic-scale structure. The essential differences are displayed in Figure 2. The salient features of the atomic arrangements in amorphous solids (also called glasses), as opposed to crystals, are illustrated in the figure for two-dimensional structures; the key points carry over to the actual three-dimensional structures of real materials. Also included in the figure, as a reference point, is a sketch of the atomic arrangement in a gas. For the sketches representing crystal (A) and glass (B) structures, the solid dots denote the fixed points about which the atoms oscillate; for the gas (C), the dots denote a snapshot of one configuration of instantaneous atomic positions.

Atomic positions in a crystal exhibit a property called long-range order or translational periodicity; positions repeat in space in a regular array, as in Figure 2A. In an amorphous solid, translational periodicity is absent. As indicated in Figure 2B, there is no long-range order.The atoms are not randomly distributed in space, however, as they are in the gas in Figure 2C. In the glass example illustrated in the figure, each atom has three nearest-neighbor atoms at the same distance (called the chemical bond length) from it, just as in the corresponding crystal. All solids, both crystalline and amorphous, exhibit short-range (atomic-scale) order .The well-defined short-range order is a consequence of the chemical bonding between atoms, which is responsible for holding the solid together.

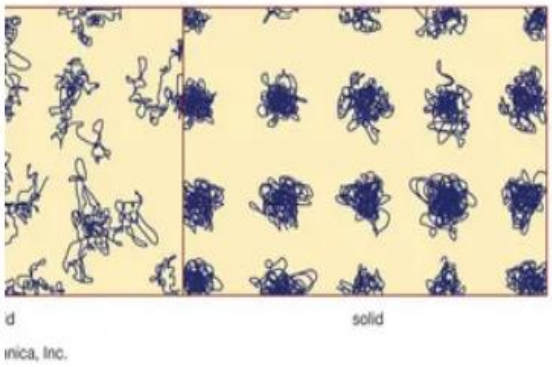

Figure 1: The state of atomic motion.
Encyclopædia Britannica, Inc.

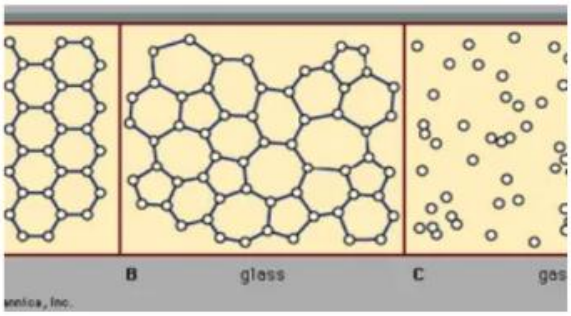

Figure 2: The atomic arrangements in (A) a crystalline solid, (B) an amorphous solid, and (C) a gas.
Encyclopædia Britannica, Inc.

In addition to the terms amorphous solid and glass, other terms in use include noncrystalline solid and vitreous solid. Amorphous solid and noncrystalline solid are more general terms, while glass and vitreous solid have historically been reserved for an

amorphous solid prepared by rapid cooling (quenching) of a melt—as in scenario 2 of Figure 3.

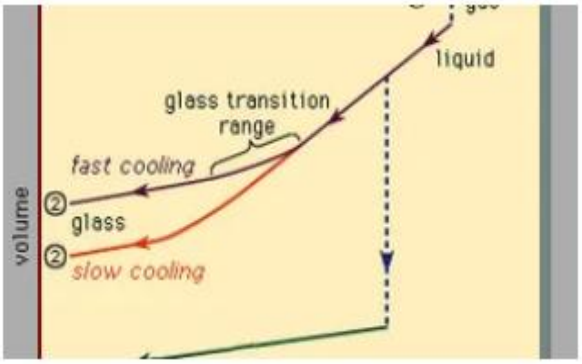

Figure 3: The two general cooling paths by which a group of atoms can condense. Route 1 is the path to the crystalline state; route 2 is the rapid-quench path to the amorphous solid state.

Encyclopædia Britannica, Inc.

Figure 3, which should be read from right to left, indicates the two types of scenarios that can occur when cooling causes a given number of atoms to condense from the gas phase into the liquid phase and then into the solid phase. Temperature is plotted horizontally, while the volume occupied by the material is plotted vertically. The temperature T is the boiling point, T is the freezing (or melting) point, and T is the glass transition temperature. In scenario 1 the liquid freezes at T into a crystalline solid, with an b f g f Figure 3: The two general cooling paths by which a group of atoms can condense. Route 1 is the path to the crystalline state; route 2 is the rapidquench path to the amorphous solid state. Encyclopædia Britannica, Inc. abrupt discontinuity in volume. When cooling occurs slowly, this is usually what happens. At sufficiently high cooling rates, however, most materials display a different behaviour and follow route 2 to the solid state. T is bypassed, and the liquid state persists until the lower temperature T is reached and the second solidification scenario is realized. In a narrow temperature range near T, the glass transition occurs: the liquid freezes into an amorphous solid with no abrupt discontinuity in volume. The glass transition temperature T is not as sharply defined as T; T shifts downward slightly when the cooling rate is reduced. The reason for this phenomenon is the steep temperature dependence of the molecular response time, which is crudely indicated by the order-of magnitude values shown along the top scale of Figure 3. When the temperature is lowered below T , the response time for molecular rearrangement becomes much larger than experimentally accessible times, so that liquidlike mobility (Figure 1, right) disappears and the atomic configuration becomes frozen into a set of fixed positions to which the atoms are tied (Figures 1, left, and 2B). Some textbooks erroneously describe glasses as undercooled viscous liquids, but this is actually incorrect. Along the section of route 2 labeled liquid in Figure 3, it is the portion lying between T and T that is correctly associated with the description of the material as an undercooled liquid (undercooled meaning that its temperature is below T). But below T , in the glass phase, it is a bona fide solid (exhibiting such properties as elastic stiffness against shear). The low slopes of the crystal and glass line segments of Figure 3 in comparison with the high slope of the liquid section reflect the fact that the coefficient of thermal expansion of a solid is small in comparison with that of the liquid

Preparation of amorphous solids: It was once thought that relatively few materials could be prepared as amorphous solids, and such materials (notably, oxide glasses and organic polymers) were called glass-forming solids. It is now known that the amorphous solid state is almost a universal property of condensable matter. The table of representative amorphous solids presents a list of amorphous solids in which every class of chemical bonding type is represented. The glass transition temperatures span a wide range.

Bonding types and glass transition temperatures of representative amorphous solids is as follows:

glass	bonding	glass transition temperature (K)
silicon dioxide	covalent	1,430
germanium dioxide	covalent	820
silicon, germanium	covalent	—
40% palladium, 40% nickel, 20% phosphorus	metallic	580
beryllium difluoride	ionic	570
arsenic trisulfide	covalent	470
polystyrene	polymeric	370
selenium	polymeric	310
80% gold, 20% silicon	metallic	290
water	hydrogen-bonded	140
ethanol	hydrogen-bonded	90
isopentane	van der Waals	65
iron, cobalt, bismuth	metallic	—

Glass formation is a matter of bypassing crystallization. The channel to the crystalline state is evaded by quickly crossing the temperature interval between T and T . Nearly all materials can, if cooled quickly enough, be prepared as amorphous solids. The definition of "quickly enough" varies enormously from material to material. These techniques are not fundamentally different from those used for preparing crystalline solids; the key is simply to quench the sample quickly enough to form the glass, rather than slowly enough to form the crystal. The quench rate increases greatly from left to right in the figure.

Melt quenching: Preparation of metallic glasses requires a quite rapid quench. It can quench a droplet of a molten metal roughly 1,000 °C in one millisecond, producing a thin film of metal that is an amorphous solid. In enormous contrast to this, the silicate glass that forms the rigid ribbed disk of the Hale telescope of the Palomar Observatory near San Diego, Calif., was prepared by cooling (over a comparable temperature drop) during a time interval of eight months. The great difference in the quench rates needed for arriving at the amorphous solid state (the quench rates here differ by a factor of 3 × 1010) is a dramatic demonstration of the difference in the glass-forming tendency of silicate glasses (very high) and metallic glasses (very low). The required quench rate for glass formation can vary significantly within a family of related materials that differ from one another in chemical composition. Au Si denotes a material containing 20 percent silicon atoms and 80 percent gold atoms.) The solid curve labeled T shows the composition dependence of the freezing point; above this line the liquid phase is the stable form. There is a deep cusp near the composition x = 0.2. Near this special composition, as at a in the figure, a liquid is much more readily quenched than is a liquid at a distant composition such as b. To reach the glass phase, the liquid must be cooled from above T to below T without crystallizing. Throughout the temperature interval from T down to the glass transition temperature T , the liquid is at risk vis-à-vis crystallization. Since this dangerous interval is much longer at b than at a, a faster quench rate is needed for glass formation at b than at a. For example, in the oxide system CaO-Al O , in which the two end-member compositions (x = 0 and x = 1) correspond to pure calcium oxide (CaO) and pure aluminum oxide (Al O), there is a deep minimum in the T -versus-x curve near the middle of the composition range. Although neither calcium oxide nor aluminum oxide readily forms a glass, glasses are easily formed from mixed compositions; for reasons related to this, many oxide glasses have complex chemical compositions.

Vapour condensation techniques: In the gold-silicon system, at compositions far from the cusp, glasses cannot be formed by melt quenching. Amorphous solids can still be prepared by dispensing with the liquid phase completely and constructing a thin solid film in atom-byatom fashion from the gas phase. A vapour stream, formed within a vacuum chamber by thermal evaporation of a sample of the material to be deposited, impinges on the surface of a cold substrate. The atoms condense on the cold surface and, under a range of conditions (usually a high rate of deposition and a low substrate temperature), an amorphous solid is formed as a thin film.

Pure silicon can be prepared as an amorphous solid in this manner. Variations of the method include using an electron beam to vaporize the source or using the plasma-induced decomposition of a molecular species. The latter technique is used to deposit amorphous silicon from gaseous silane (SiH). Among the amorphous solids listed in the table, those that normally require vapour-condensation methods for their preparation are silicon (Si), germanium (Ge), water (H O), and the elemental metallic glasses iron (Fe), cobalt (Co), and bismuth (Bi).

Other preparation techniques: Numerous other methods exist for preparing amorphous solids, and new methods are continually invented. In melt spinning, a jet of molten metal is propelled against the moving surface of a cold, rotating copper cylinder. A solid film of metallic glass is spun off as a continuous ribbon at a speed that can exceed a Kilometre per minute. In laser glazing, a brief intense laser pulse melts a tiny spot, which is swiftly quenched by the surrounding material into a glass. In sol-gel synthesis, small molecules in a liquid solution chemically link up with each other, forming a disordered network. It is possible to take a crystalline solid and convert it into an amorphous solid by bombarding it with high-kinetic-energy ions. Under certain conditions of composition and temperature, interdiffusion (mixing on an atomic scale) between crystalline layers can produce an amorphous phase. Pyrolysis and electrolysis are other methods that can be used.

Atomic-scale structure: The radial distribution function. The absence of long-range order is the defining characteristic of the atomic arrangement in amorphous solids. However, because of the absence in glasses of long parallel rows and flat parallel planes of atoms, it is extremely difficult to determine details of the atomic arrangement with the structure-probing techniques (such as X-ray diffraction) that are so successful for crystals. For glasses the information obtained from such structure-probing experiments is contained in a curve called the radial distribution function (RDF). Description for a comparison of the experimentally determined RDFs of the crystalline and amorphous forms of germanium, an elemental semiconductor similar to silicon. The heavy curve labeled a-Ge corresponds to amorphous germanium; the light curve labeled c-Ge corresponds to crystalline germanium. The significance of the RDF is that it gives the probability of neighbouring atoms being located at various distances from an average atom. The horizontal axis in the figure specifies the distance from a given atom; the vertical axis is proportional to the average number of atoms found at each distance.The curve for crystalline germanium displays sharp peaks over the full range shown, corresponding to well-defined shells of neighbouring atoms at specific distances, which arise from the long-range regularity of the crystal's atomic arrangement. Amorphous germanium exhibits a close-in sharp peak corresponding to the nearest-neighbour atoms (there are four nearest neighbours in both c-Ge and a-Ge), but at larger distances the undulations in the RDF curve become washed out owing to the absence of long-range order. The first, sharp, nearest-neighbour peak in a-Ge is identical to the corresponding peak in c-Ge, showing that the short-range order in the amorphous form of solid germanium is as well-defined as it is in the crystalline form. The normal procedure is to construct a model of the structure and then to calculate from the model's atomic positions a theoretical RDF curve. This calculated RDF is then compared to the experimental curve (which provides the definitive test of the validity of the model). Computer-assisted refinements are then made in the model in order to improve the agreement between the model-dependent theoretical RDF and the experimentally observed RDF. This program has been successfully carried out for many amorphous solids, so there is now much that is known about their atomic-scale structure. In contrast to the complete information available for crystals, however, the structural knowledge of glasses still contains gaps (42).

Formation: The production of amorphous ice hinges on the fast rate of cooling. Liquid water must be cooled to its glass transition temperature (about 136 K or −137 °C) in milliseconds to prevent the spontaneous nucleation of crystals. Pressure is another important factor in the formation of amorphous ice, and changes in pressure may cause one form to convert into another. Contents Formation Cryoprotectants can be added to water to lower its freezing point (like antifreeze) and increase viscosity, which inhibits the formation of crystals. Vitrification without addition of cryoprotectants can be achieved by very rapid cooling. These techniques are used in biology for cryopreservation of cells and tissues.

Low-density amorphous ice:Low-density amorphous ice, also called LDA, vapor-deposited amorphous water ice or amorphous solid water (ASW) is usually formed in the laboratory by a slow accumulation of water vapor molecules (physical vapor deposition) onto a very smooth metal crystal surface under 120 K. In outer space it is expected to be formed in a similar manner on a variety of cold substrates, such as dust particles. Melting past its glass transition temperature (Tg) between 120 and 140 K, LDA is more viscous than normal water. Recent studies have shown the viscous liquid stays in this alternative form of liquid water up to somewhere between 140 and 210 K, a temperature range that is also inhabited by ice Ic . LDA has a density of 0.94 g/cm3, less dense than the densest water (1.00 g/cm3 at 277 K), but denser than ordinary ice (ice Ih). By contrast, hyperquenched glassy water (HGW) is formed by spraying a fine mist of water droplets into a liquid such as propane around 80 K, or by hyperquenching fine micrometer-sized droplets on a sample-holder kept at liquid nitrogen temperature, 77 K, in a vacuum. Cooling rates above 104 K/s are required to prevent crystallization of the droplets. At liquid nitrogen temperature, 77 K, HGW is kinetically stable and can be stored for many years.

High-density amorphous ice: High-density amorphous ice (HAD) can be formed by compressing ice Ih at temperatures below ~140 K. At 77 K, HAD forms from ordinary natural ice at around 1.6 Gpa and from LDA at around 0.5 Gpa[7] (approximately 5,000 atm). At this temperature, it can be recovered back to ambient pressure and kept indefinitely. At these conditions (ambient pressure and 77 K), HAD has a density of 1.17 g/cm3. Peter Jenniskens and David F. Blake demonstrated in 1994 that a form of high-density amorphous ice is also created during vapor deposition of water on low-temperature (< 30 K) surfaces such as interstellar grains. The water molecules do not fully align to create the open cage structure of lowdensity amorphous ice. Many water molecules end up at interstitial positions. When warmed above 30 K, the structure re-aligns and transforms into the low-density form.

Very-high-density amorphous ice: Very-high-density amorphous ice (VHDA) was discovered in 1996 by Osamu Mishima who observed that HAD became denser if warmed to 160 K at pressures between 1 and 2 Gpa and has a density of 1.26 g/cm3 at ambient pressure and temperature of 77 K. More recently it was suggested that this denser amorphous ice was a third amorphous form of water, distinct from HAD, and was named VHDA

Amorphous ice in the Solar SystemProperties: In general, amorphous ice can form below ~130 K. At this temperature, water molecules are unable to form the crystalline structure commonly found on Earth. Amorphous ice may also form in the coldest region of the Earth's atmosphere, the summer polar mesosphere, where noctilucent clouds exist. These low temperatures are readily achieved in astrophysical environments such as molecular clouds, circumstellar disks, and the surfaces of objects in the outer solar system. In the laboratory, amorphous ice transforms into crystalline ice if it is heated above 130 K, although the exact temperature of this conversion is dependent on the

environment and ice growth conditions. The reaction is irreversible and exothermic, releasing 1.26–1.6 kJ/mol. An additional factor in determining the structure of water ice is deposition rate. Even if it is cold enough to form amorphous ice, crystalline ice will form if the flux of water vapor onto the substrate is less than a temperature-dependent critical flux. This effect is important to consider in astrophysical environments where the water flux can be low. Conversely, amorphous ice can be formed at temperatures higher than expected if the water flux is high, such as flash-freezing events associated with cryovolcanism. At temperatures less than 77 K, irradiation from ultraviolet photons as well as high-energy electrons and ions can damage the structure of crystalline ice, transforming it into amorphous ice. Amorphous ice does not appear to be significantly affected by radiation at temperatures less than 110 K, though some experiments suggest that radiation might lower the temperature at which amorphous ice begins to crystallize.

Detection: Amorphous ice can be separated from crystalline ice based on its near-infrared and infrared spectrum. At near-IR wavelengths, the characteristics of the 1.65, 3.1, and 4.53 μm water absorption lines are dependent on the ice temperature and crystal order. The peak strength of the 1.65 μm band as well as the structure of the 3.1 μm band are particularly useful in identifying the crystallinity of water ice. At longer IR wavelengths, amorphous and crystalline ice have characteristically different absorption bands at 44 and 62 μm in that the crystalline ice has significant absorption at 62 μm while amorphous ice does not. In addition, these bands can be used as a temperature indicator at very low temperatures where other indicators (such as the 3.1 and 12 μm bands) fail. This is useful studying ice in the interstellar medium and circumstellar disks. However, observing these features is difficult because the atmosphere is opaque at these wavelengths, requiring the use of space-based infrared observatories.

Molecular clouds, circumstellar disks, and the primordial solar nebula: Molecular clouds have extremely low temperatures (~10 K), falling well within the amorphous ice regime. The presence of amorphous ice in molecular clouds has been observationally confirmed. When molecular clouds collapse to form stars, the temperature of the resulting circumstellar disk isn't expected to rise above 120 K, indicating that the majority of the ice should remain in an amorphous state. However, if the temperature rises high enough to sublimate the ice, then it can re-condense into a crystalline form since the water flux rate is so low. This is expected to be the case in the circumstellar disk of IRAS 09371+1212, where signatures of crystallized ice were observed despite a low temperature of 30–70 K. Properties Detection Molecular clouds, circumstellar disks, and the primordial solar nebula For the primordial solar nebula, there is much uncertainty as to the crystallinity of water ice during the circumstellar disk and planet formation phases. If the original amorphous ice survived the molecular cloud collapse, then it should have been preserved at heliocentric distances beyond Saturn's orbit (~12 AU)

Comets: Evidence of amorphous ice in comets is found in the high levels of activity observed in long-period, Centaur, and Jupiter Family comets at heliocentric distances beyond ~6 AU. These objects are too cold for the sublimation of water ice, which drives comet activity closer to the sun, to have much of an effect. Thermodynamic models show that the surface temperatures of those comets are near the amorphous/crystalline ice transition temperature of ~130 K, supporting this as a likely source of the activity. The runaway crystallization of amorphous ice can produce the energy needed to power outbursts such as those observed for Centaur Comet 29P/Schwassmann– Wachmann

Kuiper Belt objects: With radiation equilibrium temperatures of 40–50 K, the objects in the Kuiper Belt are expected to have amorphous water ice. While water ice

has been observed on several objects, the extreme faintness of these objects makes it difficult to determine the structure of the ices. The signatures of crystalline water ice were observed on 50000 Quaoar, perhaps due to resurfacing events such as impacts or cryovolcanism.

Icy moons: The Near-Infrared Mapping Spectrometer (NIMS) on NASA's Galileo spacecraft spectroscopically mapped the surface ice of the Jovian satellites Europa, Ganymede, and Callisto. The temperatures of these moons range from 90–160 K, warm enough that amorphous ice is expected to crystallize on relatively short timescales. However, it was found that Europa has primarily amorphous ice, Ganymede has both amorphous and crystalline ice, and Callisto is primarily crystalline. This is thought to be the result of competing forces: the thermal crystallization of amorphous ice versus the conversion of crystalline to amorphous ice by the flux of charged particles from Jupiter. Closer to Jupiter than the other three moons, Europa receives the highest level of radiation and thus through irradiation has the most amorphous ice. Callisto is the farthest from Jupiter, receiving the lowest radiation flux and therefore maintaining its crystalline ice. Ganymede, which lies between the two, exhibits amorphous ice at high latitudes and crystalline ice at the lower latitudes. This is thought to be the result of the moon's intrinsic magnetic field, which would funnel the charged particles to higher latitudes and protect the lower latitudes from irradiation. The surface ice of Saturn's moon Enceladus was mapped by the Visual and Infrared Mapping Spectrometer (VIMS) on the NASA/ESA/ASI Cassini space probe. The probe found both crystalline and amorphous ice, with a higher degree of crystallinity at the "tiger stripe" cracks on the surface and more amorphous ice between these regions. The crystalline ice near the tiger stripes could be explained by higher temperatures caused by geological activity that is the suspected cause of the cracks. The amorphous ice might be explained by flash freezing from cryovolcanism, rapid condensation of molecules from water geysers, or irradiation of high-energy particles from Saturn.

Earth's polar mesosphere: Ice clouds form at and below the Earth's high latitude mesopause (~90 km) where temperatures have been observed to fall as to below 100 K. It has been suggested that homogeneous nucleation of ice particles results in low density amorphous ice. Amorphous ice is likely confined to the coldest parts of the clouds and stacking disordered ice I is thought to dominate elsewhere in these polar mesospheric clouds

Uses: Amorphous ice is used in some scientific experiments, especially in cryo-electron microscopy of biomolecules. The individual molecules can be preserved for imaging in a state close to what they are in liquid water.

REFERENCES

Amann-Winkel, K.; Bellissent-Funel, M. C.; Bove, L. E.; Loerting, T.; Nilsson, A.; Paciaroni, A.; Schlesinger, D.; Skinner, L.2016. X-Ray and Neutron Scattering of Water. Chem. Rev. 116: 7570– 7589.

Amann-Winkel, K.; Böhmer, R.; Fujara, F.; Gainaru, C.; Geil, B.; Loerting, T.2016. Colloquium: Water’s Controversial Glass Transitions. Rev. Mod. Phys., 88: 011002.

Amann-Winkel, K.; Böhmer, R.; Fujara, F.; Gainaru, C.; Geil, B.; Loerting, T.2016. Colloquium: Water’s Controversial Glass Transitions. Rev. Mod. Phys., 88: 011002.

Amorphous Solids, Encyclopaedia Britannica. 2019. solid solution | chemistry | Britannica

Bar-Nun, A.; Dror, J.; Kochavi, E.; Laufer, D. 1987. Amorphous Water Ice and Its Ability to Trap Gases. Phys. Rev. B, 35: 2427.

Bossa, J. B.; Isokoski, K.; De Valois, M. S.; Linnartz, H. 2012. Thermal Collapse of Porous Interstellar Ice. Astron. Astrophys., 545, A82.

Bowron, D. T.; Finney, J. L.; Hallbrucker, A.; Kohl, I.; Loerting, T.; Mayer, E.; Soper, A. K. 2006. The Local and

Intermediate Range Structures of the Five Amorphous Ices at 80 K and Ambient Pressure: A Faber-Ziman and Bhatia-Thornton Analysis. J. Chem. Phys., 125: 194502.

Burton, E. F.; Oliver, W. F.1935. X-Ray Diffraction Patterns of Ice. Nature, 135: 505– 506.

Burton, E. F.; Oliver, W. F. 1975. Amorphous Solid Water. Phys. Bull., 26: 211– 211.

Cartwright, J. H. E.; Escribano, B.; Sainz-Diaz, C. I. 2008. The Mesoscale Morphologies of Ice Films: Porous and Biomorphic Forms of Ice under Astrophysical Conditions. Astrophys. J., 687:1406– 1414.

Cholette, F.; Zubkov, T.; Smith, R. S.; Dohnálek, Z.; Kay, B. D.; Ayotte, P. Infrared Spectroscopy and Optical Constants of Porous Amorphous Solid Water. J. Phys. Chem. B 2009, 113, 4131–4140.

De Barros, A. L. F.; Boduch, P.; Domaracka, A.; Rothard, H.; Da Silveira, E. F. 2012. Radiolysis of Astrophysical Ices by Heavy Ion Irradiation: Destruction Cross Section Measurement. Low Temp. Phys., 38: 759–765.

Ehrenfreund, P.; Fraser, H. J.; Blum, J.; Cartwright, J. H. E.; García-Ruiz, J. M.; Hadamcik, E.; Levasseur-Regourd, A. C.; Price, S.; Prodi, F.; Sarkissian, A. 2003. Physics and Chemistry of Icy Particles in the Universe: Answers from Microgravity. Planet. Space Sci., 51: 473– 494.

Fredon, A.; Groenenboom, G. C.; Cuppen, H. M. 2021. Molecular Dynamics Simulations of Energy Dissipation on Amorphous Solid Water: Testing the Validity of Equipartition. ACS Earth Space Chem., 5: 2032– 2041.

Gärtner, S.; Headen, T. F.; Youngs, T. G. A.; Hill, C. R.; Pascual, N.; Auriacombe, O.; Ioppolo, S.; Loerting, T.; Bowron, D. T.; Fraser, H. J.2019. Nanoscale Structure of Amorphous Solid Water: What Determines the Porosity in ASW?. Proc. Int. Astron. Union, 15: 368– 369.

Ghormley, J. A.; Hochanadel, C. J. Amorphous Ice: Density and Reflectivity. Science 1971, 171: 62– 64.

Hagen, W.; Tielens, A. G. G. M.1982. The Librational Region in the Spectrum of Amorphous Solid Water and Ice Ic between 10 and 140 K. Spectrochim. Acta, Part A, 38: 1089– 1094.

Hill, C. R.; Mitterdorfer, C.; Youngs, T. G. A.; Bowron, D. T.; Fraser, H. J.; Loerting, T. 2016. Neutron Scattering Analysis of Water's Glass Transition and Micropore Collapse in Amorphous Solid Water. Phys. Rev. Lett., 116: 215501.

Jenniskens, P.; Blake, D. F. 1994. Structural Transitions in Amorphous Water Ice and Astrophysical Implications. Science, 265: 753– 756.

Jenniskens, P.; Blake, D. F.; Wilson, M. A.; Pohorille, A.1995. High-Density Amorphous Ice, the Frost on Interstellar Grains. Astrophys. J., 455: 389– 401.

Journal of physical chemistry, ISSN : 1520-5207, Publisher: American Chemical Society, "Volatility of Amorphous Solid Water"@eng.

Kouchi, A.; Kuroda, T. 1990. Amorphization of cubic ice by ultraviolet irradiation. Nature, 344: 134– 135.

Loerting, T.; Bauer, M.; Kohl, I.; Watschinger, K.; Winkel, K.; Mayer, E.2011. Cryoflotation: Densities of Amorphous and Crystalline Ices. J. Phys. Chem. B, 115: 14167– 14175.

May, R. A.; Smith, R. S.; Kay, B. D. 2011. Probing the Interaction of Amorphous Solid Water on a Hydrophobic Surface: Dewetting and Crystallization Kinetics of ASW on Carbon Tetrachloride. Phys. Chem. Chem. Phys., 13: 19848– 19855.

Mayer, E.; Pletzer, R.1986. Astrophysical Implications of Amorphous Ice - A Microporous Solid. Nature, 319: 298–301.

Mejía, C.; de Barros, A. L. F.; Seperuelo Duarte, E.; da Silveira, E. F.; Dartois, E.; Domaracka, A.; Rothard, H.; Boduch, P.2015. Compaction of Porous Ices Rich in Water by Swift Heavy Ions. Icarus, 250: 222– 229.

Mitterdorfer, C.; Bauer, M.; Youngs, T. G. A.; Bowron, D. T.; Hill, C. R.; Fraser, H. J.; Finney, J. L.; Loerting, T.2014. Small-Angle Neutron Scattering Study of Micropore Collapse in Amorphous Solid Water. Phys. Chem. Chem. Phys., 16: 16013– 16020.

Noble, J. A.; Cuppen, H. M.; Coussan, S.; Redlich, B.; Ioppolo, S.2020. Infrared Resonant Vibrationally Induced Restructuring of Amorphous Solid Water. J. Phys. Chem. C, 124: 20864– 20873.

Noble, J. A.; Martin, C.; Fraser, H. J.; Roubin, P.; Coussan, S.2014. Unveiling the Surface Structure of Amorphous Solid Water via Selective Infrared Irradiation of OH Stretching Modes. J. Phys. Chem. Lett., 5: 826– 829.

Oba, Y.; Miyauchi, N.; Hidaka, H.; Chigai, T.; Watanabe, N.; Kouchi, A. 2009. Formation of Compact Amorphous H2O Ice by Codeposition of Hydrogen Atoms with Oxygen Molecules on Grain Surfaces. Astrophys. J., 701: 464– 470.

Raut, U.; Famá, M.; Loeffler, M. J.; Baragiola, R. A.2008. Cosmic Ray Compaction of Porous Interstellar Ices. Astrophys. J., 687: 1070– 1074.

Shalit, A.; Perakis, F.; Hamm, P.2014. Communication: Disorder-Suppressed Vibrational Relaxation in Vapor-Deposited High-Density Amorphous Ice. J. Chem. Phys., 140: 151102.

Shephard, J. J.; Evans, J. S. O.; Salzmann, C. G. 2013. Structural Relaxation of Low-Density Amorphous Ice upon Thermal Annealing. J. Phys. Chem. Lett., 4: 3672– 3676.

Smith, R. S.; Huang, C.; Kay, B. D. 1997. Evidence for Molecular Translational Diffusion during the Crystallization of Amorphous Solid Water. J. Phys. Chem. B, 101: 6123– 6126.

Smith, R. S.; Kay, B. D. 1999. The Existence of Supercooled Liquid Water at 150 K. Nature, 398: 788– 791.

Smith, R. S.; Matthiesen, J.; Knox, J.; Kay, B. D. 2011. Crystallization Kinetics and Excess Free Energy of H2O and D2O Nanoscale Films of Amorphous Solid Water. J. Phys. Chem. A, 115: 5908– 5917.

Smith, R. S.; Yuan, C.; Petrik, N. G.; Kimmel, G. A.; Kay, B. D. 2019. Crystallization Growth Rates and Front Propagation in Amorphous Solid Water Films. J. Chem. Phys., 214703.

Smith, R. S.; Zubkov, T.; Dohnálek, Z.; Kay, B. D. 2009. The Effect of the Incident Collision Energy on the Porosity of Vapor-Deposited Amorphous Solid Water Films. J. Phys. Chem. B, 113: 4000– 4007.

Stevenson, K. P.; Kimmel, G. A.; Dohnálek, Z.; Smith, R. S.; Kay, B. D. 1999. Controlling the Morphology of Amorphous Solid Water. Science, 283: 1505– 1507.

Tulk, C. A.; Benmore, C. J.; Urquidi, J.; Klug, D. D.; Neuefeind, J.; Tomberli, B.; Egelstaff, P. A.2002. Structural Studies of Several Distinct Metastable Forms of Amorphous Ice. Science, 297: 1320– 1323.

Venkatesh, C. G.; Rice, S. A.; Narten, A. H.1974. Amorphous Solid Water: An x-Ray Diffraction Study. Science, 186: 927– 928.

Yuan, C.; Smith, R. S.; Kay, B. D. 2017. Communication: Distinguishing between Bulk and Interface-Enhanced Crystallization in Nanoscale Films of Amorphous Solid Water. J. Chem. Phys., 146: 031102.